

## Chapter 7: Finite Element Analysis and Applications to MEMS

J. Newell , K. Man, and B. Stark

The design and development of MEMS is a challenging task, requiring substantial investment in capital equipment and plant facilities. For such investments to be fruitful, MEMS engineers must have the capability to fully characterize the inner workings of these devices, in order to predict temperatures, stresses, dynamic response characteristics, and possible failure mechanisms. Relatively simple hand calculations can often be performed for such analyses, particularly when considering planar or beam-type geometries subject to the influence of temperature, applied force, or pressure loads. These analyses were presented in the preceding chapter for individual devices. The finite element method provides a convenient tool for conducting more complex analyses, and will be discussed in some detail.

In finite element analysis, the structure to be analyzed is discretized into small elements, each having an associated stiffness matrix. Several finite elements have been developed to represent common structures, including quadrilateral plates, triangular plates, solid brick elements, and beam elements. For each such element, the stiffness matrix is stored mathematically in a lookup table, in the form of fundamental equations. When problem-specific parameters such as dimensional coordinates, the material elastic modulus, Poisson's ratio and density are put in these equations, the local stiffness, as represented by one element, is uniquely known. When a structure is fully discretized, or meshed, into many such elements, its global stiffness can be assembled, again in the form of a matrix, from the combined stiffnesses of all the interacting elements. If a force or set of forces is subsequently applied to the structure, the static displacement response can then be calculated by inverting the global stiffness matrix, as follows:

$$\{F\} = \{k\}\{x\} \Rightarrow \{x\} = \{F\}\{k\}^{-1} \quad (7-1)$$

where  $\{F\}$  = applied force vector

$\{k\}$  = stiffness matrix

$\{x\}$  = displacement vector.

This basic concept can be used in the solution of many problems involving a variety of applied loading conditions, including externally applied static forces, pressures and temperatures. Several example cases of such analyses are provided below.

## I. Heat Transfer Analysis

Finite element models are often used to study the heat transfer characteristics of a device, to understand where and how heat is rejected as well as the transient and steady-state temperature distributions. Figure 7-1 shows such a finite element model of an advanced hybrid, where unpackaged die are bonded to a chip carrier substrate.

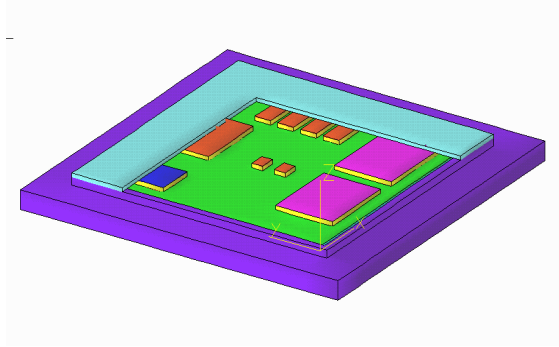


**Figure 7-1: Hybrid device with cover removed.**

When the device is powered, the die reject a known amount of power. The temperature increase through the stack of materials from the top of the chip to the bottom of the package is evaluated, along with the temperature distribution within the various layers. This identifies any potential limitations due to adhesive or dielectric material selection.

Another example of a heat transfer analysis is illustrated in Figure 7-2, which shows a solid model of a substrate-mounted die. In this model, the die is bonded to a substrate with an adhesive, and the substrate is in turn bonded to a steel header. When the die-generated heat flux is applied to the model, the steady state temperature distribution, shown in the figure, occurs.

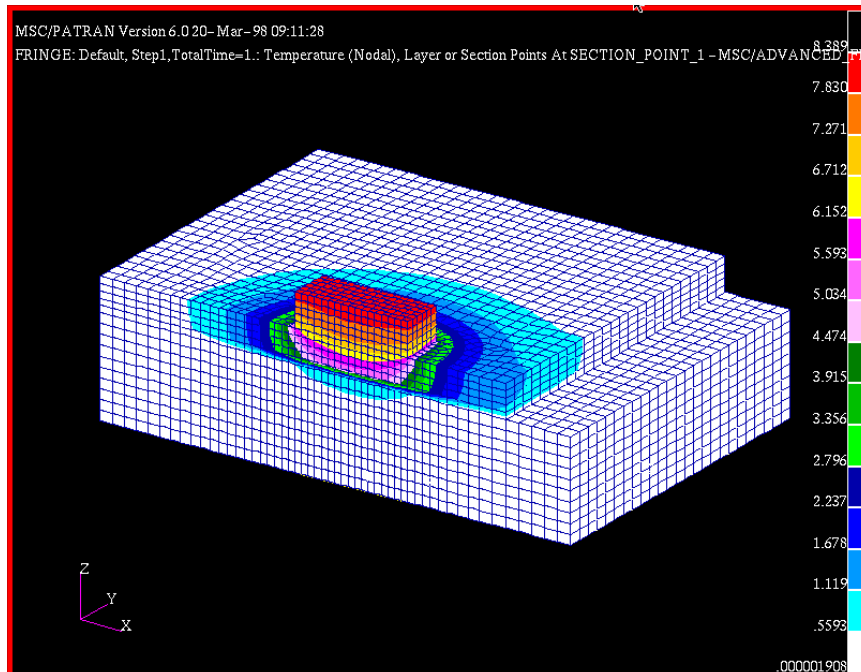


**Figure 7-2: Substrate mounted die.**

This modeling can be applied to aid in MEMS design. One example of this was done in the development of a microisolation valve for future spacecraft propulsion systems. To do this, a model was created to study temperature distributions in a channel barrier upon application of device power. The geometry of Figure 7-3 was used to create the model of heat distribution, which was analytically loaded with a known power input. The finite element analysis resulted in Figure 7-4, which shows temperature distribution at discrete locations on the valve.

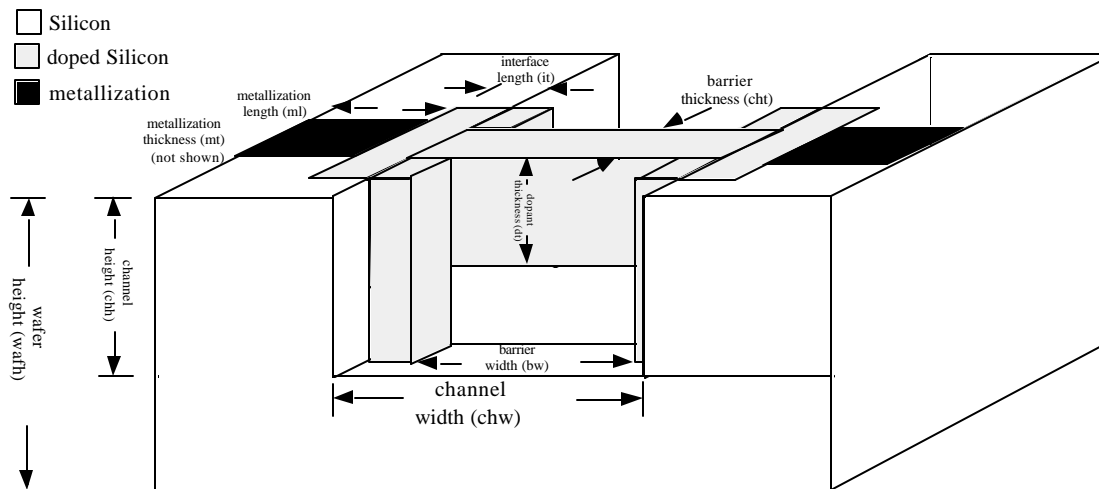


**Figure 7-3: Channel barrier schematic.**

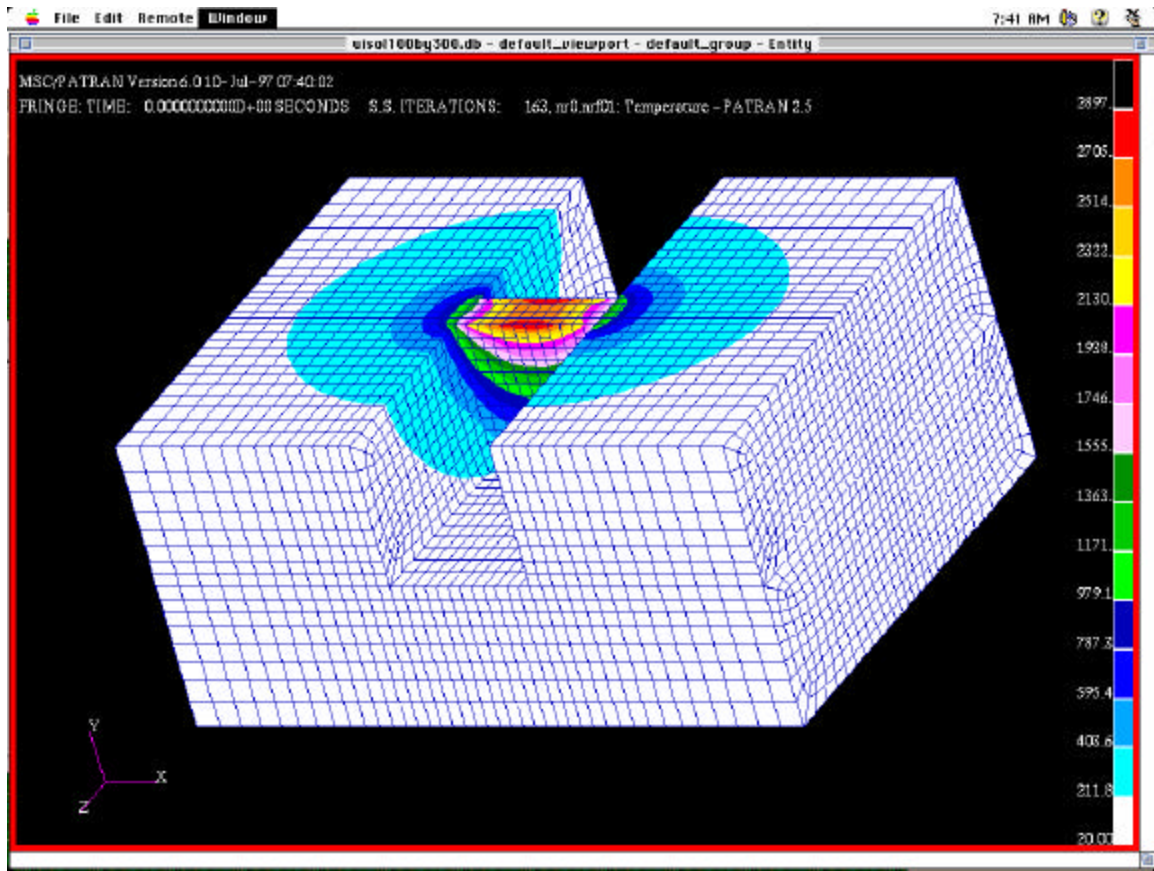


**Figure 7-4: Temperature distribution in channel barrier.**

## **II. Thermal Stress Analysis**

Finite element modeling can also be used to model thermal stress. Figure 7-4 shows an etched recess in silicon, part of another micropropulsion system, which is used to reduce heat loss into the structure by creating a thermal choke near the edge of the heater strips. The thermal and structural finite element models used to assess the heat loss associated with the geometry of the structure are shown on the right. They show a dramatic reduction in heat loss by decreasing the cross sectional area through which heat flux occurs and by increasing the heat conductive path. However, there is a limit to which the bridge thickness can be reduced without compromising its structural integrity. Through these applications of finite element analyses, it is possible to obtain a nearly optimum design.

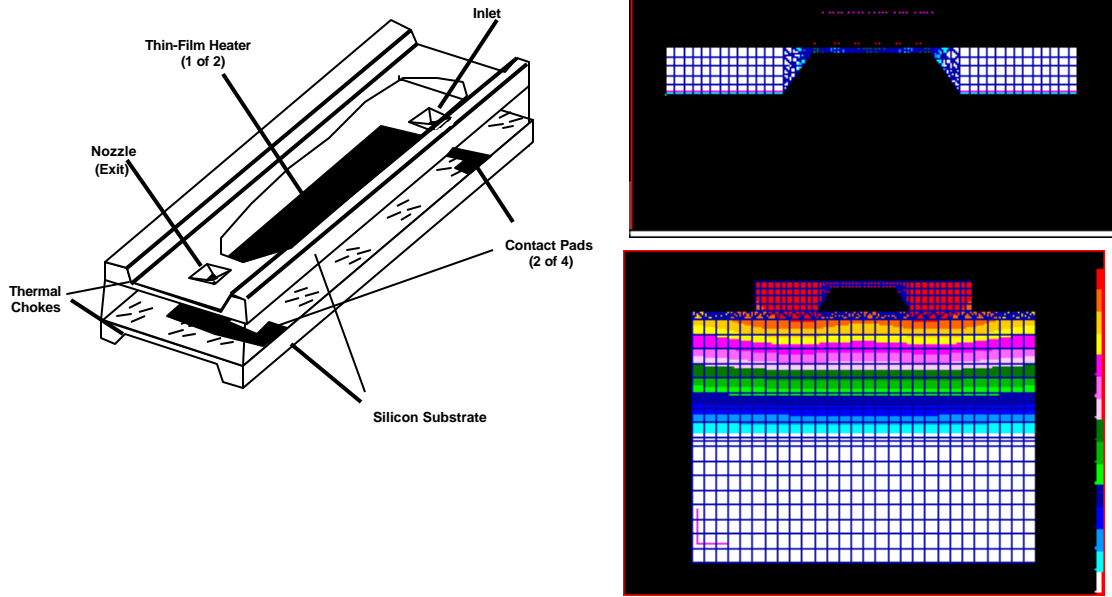


Figure 7-5: Finite element model of a vaporizing liquid microthruster.

### III. Thermal Fatigue Stress Analysis

Another application of finite element analysis is examining the effects of thermal fatigue. When structural members are subjected to repeated loading, failure can occur at stresses significantly lower than the ultimate tensile strength of the material, as discussed in Chapter 3. In a fatigue situation, the designer or engineer would generally like to predict the number of cycles a member can endure prior to failure. A widely used technique for such predictions is the Coffin-Manson relation:[60]

$$\frac{\Delta \epsilon}{2} = \frac{\sigma_f'}{E} (2N_f)^b + \epsilon_f' (2N_f)^c \quad (7-2)$$

where

$\Delta \epsilon$  is the total cyclic strain excursion,

$\sigma_f'$  is the fatigue strength coefficient,

$2N_f$  is the number of load reversals to failure,

$b$  is the fatigue strength exponent,

$\epsilon'_f$  is the fatigue ductility coefficient,

$c$  is the fatigue ductility exponent.

The four fatigue parameters  $\sigma'_f$ ,  $\epsilon'_f$ ,  $b$  and  $c$  must be determined from experimental cycle test data, and are documented in the literature for many materials. The usefulness of this equation comes from the fact that, when the cyclic strain excursion, elastic modulus and four fatigue parameters are known, the number of load reversals to failure  $2N_f$  can be calculated.

This analysis can be facilitated through finite element modeling, and an example of the thermal stresses occurring in microelectronic device vias is offered. The via is an aluminum trace embedded in a parent silicon substrate, which serves as a conductive path to facilitate signal flow from one location to another within the device. When the chip is powered, internally dissipated heat elevates the device temperature, inducing thermal stresses in regions of dissimilar material. These stresses, produced by mismatches in the local coefficient of thermal expansion, are important parameters to understand, as they directly affect the life of the device.

Figure 7-6 shows a 3-dimensional electron microscope image of the structure under study. If a cross-section is taken through the Figure 7-6 via, the geometry illustrated in Figure 7-7 is found. The typical via has a slope of 26 degrees, with sharp intersecting corners at signal plane transitions.

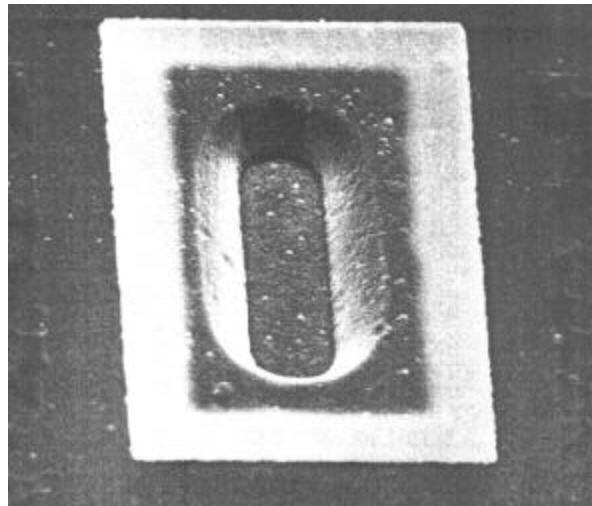
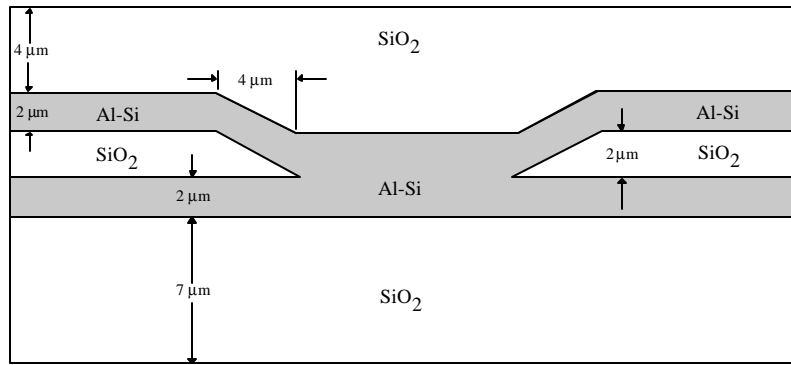


Figure 7-6: Electron micrograph of 3-D intermetallic via.



**Figure 7-7: Inter-metallization via geometry.**

The device must operate in a severe environment, with temperatures ranging from -65 °C to 150 °C. Such a large temperature excursion causes significant stress in the materials, due primarily to the difference in coefficients of thermal expansion between the metal layers and the SiO<sub>2</sub> dielectric. The stress problem is made even worse through duty cycling, in which the unit is powered on and off repeatedly, forcing the via to undergo cyclic stress-strain excursions.

To effect a calculation of the total cyclic strain range, the device cross-section was used in the construction of a 2-dimensional, plane strain finite element model. As illustrated in Figure 7-8, the finalized FEM incorporated 702 two-dimensional elements, connecting a total of 758 space coordinates. A vertical constraint boundary condition was placed on nodes of the base silicon dioxide layer, while a symmetry argument was invoked on the two sides. The top of the passivation layer was allowed to expand without restraint.

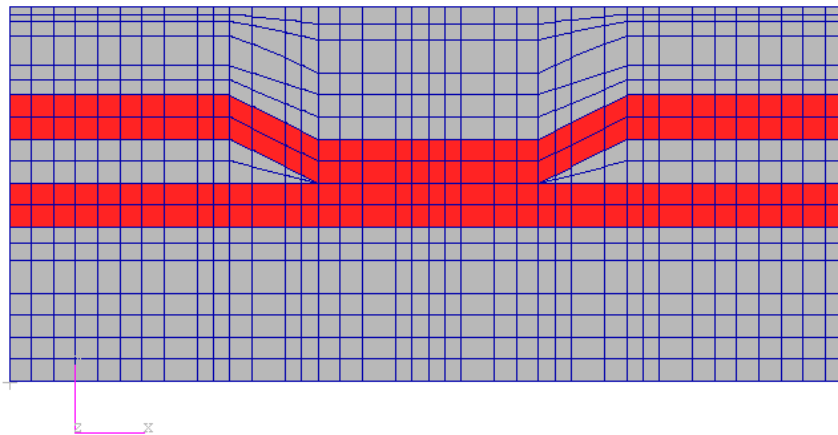


**Figure 7-8: Finite element model of intermetallic via.**

To obtain the cyclic stress-strain response, a temperature field was applied to the model to simulate repeated heat-up and cool-down cycling between temperatures of -65 °C and 150 °C. The resulting non-linear, elasto-plastic stress-strain response was obtained, assuming a von Mises yield criterion.

Figure 7-9 shows a plot of maximum von Mises equivalent stress versus equivalent strain from the finite element model. The output was requested at a single space coordinate, whose stress-strain response was larger than at any other model location.

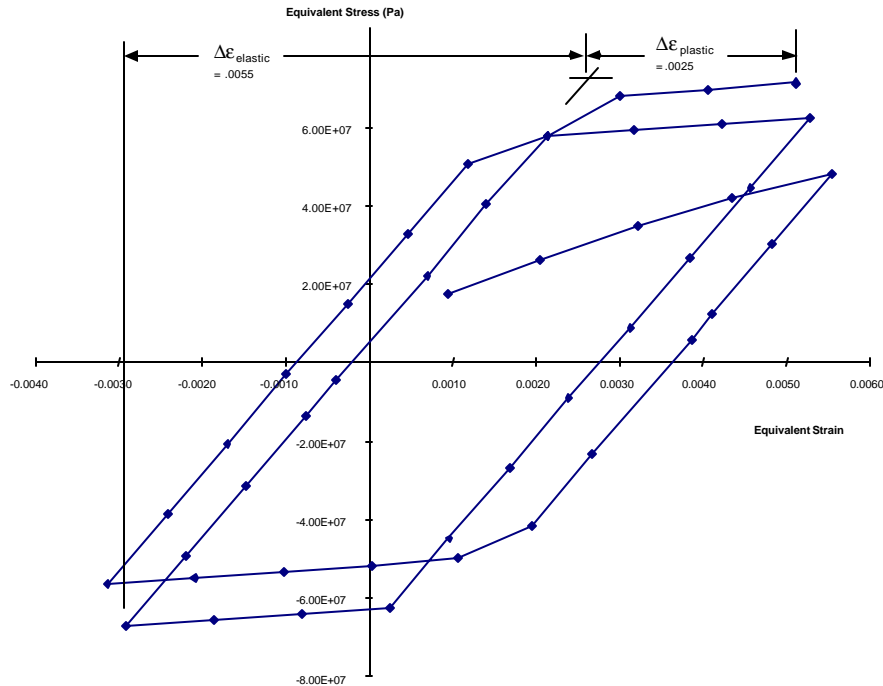


**Figure 7-9: Stress-strain hysteresis loop from finite element analysis.**

The plot shows a total of 5 temperature cycles, and illustrates a number of interesting facts. Nonlinearity of the via material is evident, with yielding seen to occur at the outset of the initial temperature rise, and subsequently at various points in hot/cold cycling. The material also undergoes strain hardening during each cycle such that, with each subsequent temperature loop, a slightly higher stress is required to develop the same strain. The material response tends to stabilize with each successive load reversal, until a relatively stable hysteresis loop is achieved.

By examining the last, ostensibly stable hysteresis loop, the total cyclic strain range is seen to equal approximately 0.008, with elastic and plastic components as indicated in Figure 7-10. With the cyclic strain range determined, device life can be calculated from Equation 7-2. For additional information regarding these techniques, the reader is referred to References [60] and [62].

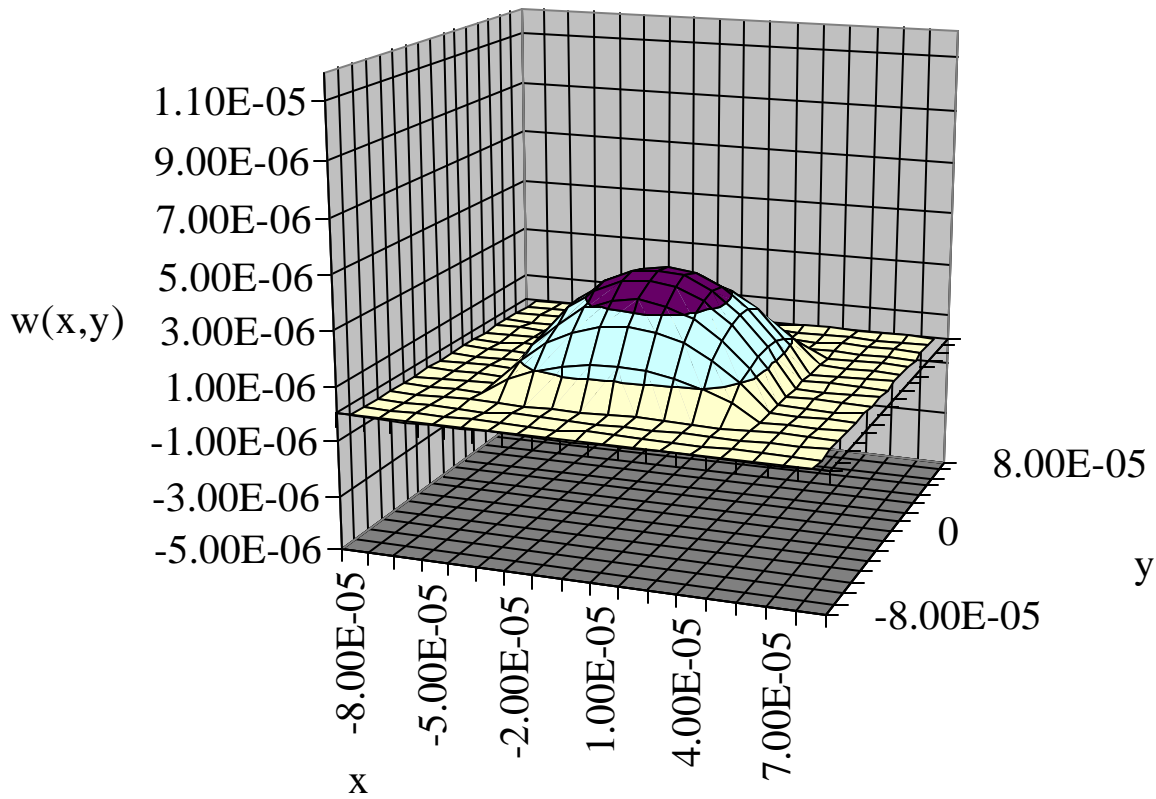


Figure 7-10: Static deflection of a 3 mm thick Si membrane subjected to a 1 MPa pressure.

#### IV. Static Analysis

One of the more common uses of finite element modeling is to look at the static motion of mechanical objects. As presented in Chapter 6, motion becomes very difficult to analytically determine as structures become arbitrarily complex. For this reason, finite element modeling can be used to determine the mechanical response of structures to external forces.

One common application of static analysis is in the deflection of thin plates. Application of finite element modeling yields the result for a square plate of width  $a$ , with fixed boundary conditions, that the deflection of the center of the plate,  $w_0$ , is approximated by:

$$w_0 = \frac{qa^4}{256D} \quad (7-3)$$

where

$q$  = uniformly distributed load

$D$  = flexural rigidity of the membrane

If this method is applied to the entire plate, it will yield a deflection shown in Figure 7-10.

## V. Modal Analysis

Another application of finite element modeling to MEMS is the analysis of resonant modes. Modal information is useful because a) it shows displacement maxima in a vibration event, b) it reveals the frequencies of natural vibration, and it can be used to predict the stochastic response of the device when it is excited by random vibration, as occurs during a spacecraft launch. Figures 7-12 and 7-13 show the resulting shapes of two such modes in the device shown in Figure 6-8. It should be noted that these are naturally occurring resonant excitation states of the device, and will be excited if a harmonic forcing function is applied to the unit.

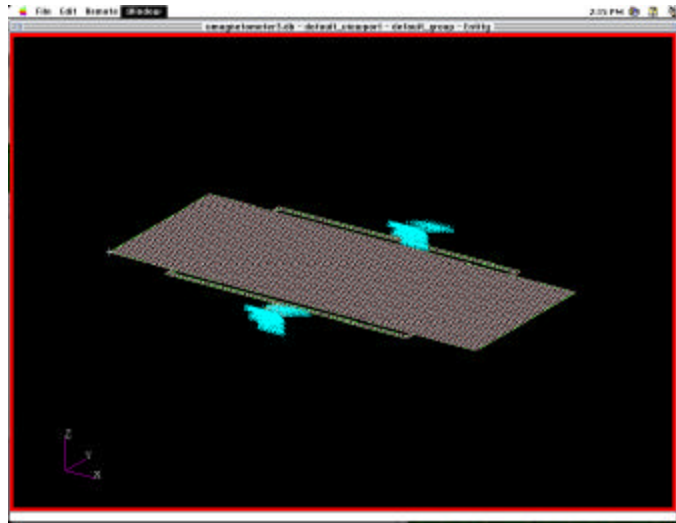


Figure 7-11: Finite element model of a micromagnetometer.

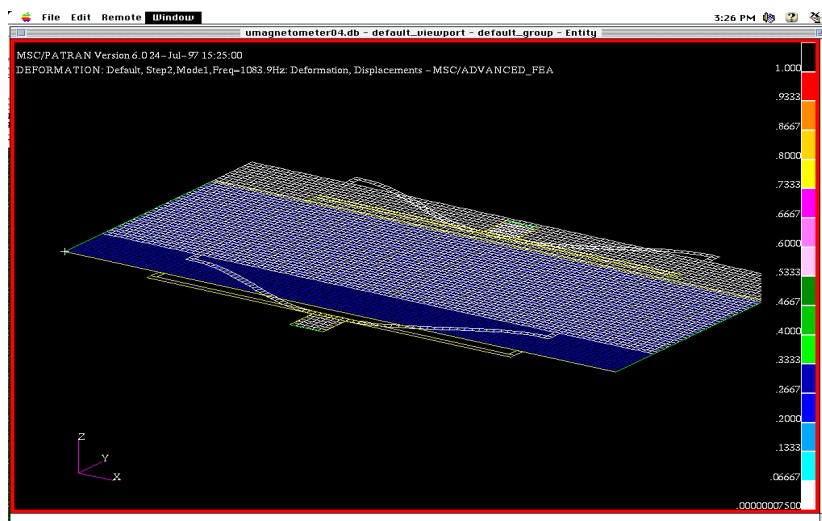


Figure 7-12: 1st resonant mode.

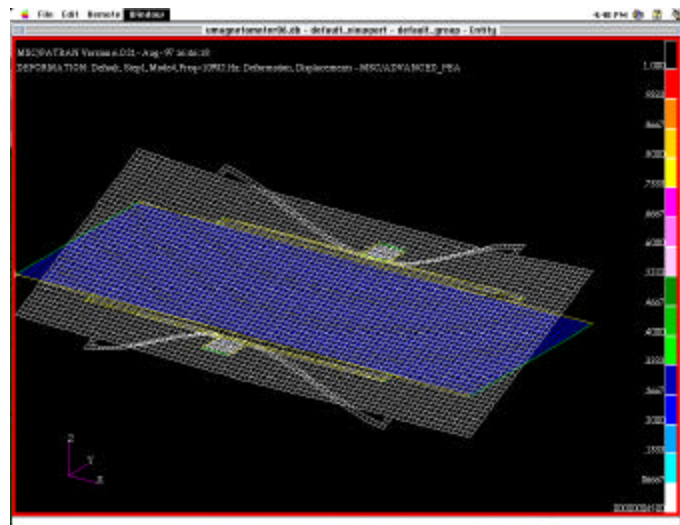


Figure 7-13: 2nd resonant mode.

## VI. Software Tools

Many software tools are available for general finite element analysis, and information regarding a number of these is included in the table below. Note that virtually all such packages provide linear static, dynamic and normal modes analysis capabilities. PATRAN and I-DEAS both have highly evolved user interfaces, and are most suitable for pre- and post-processing of finite element models, regardless of the FE solver utilized. ABAQUS and ANSYS are known for their strong capabilities in highly non-linear analysis. Both COSMOS and FEMAP are PC-based codes, designed for optimum performance on Windows-based personal computers. Cosmic NASTRAN is a public-domain code developed by NASA in the 1960s. As such, it comes with few features, but is available at very low cost.

Software Package	Capabilities	Vendor
Cosmic NASTRAN	Linear statics, dynamics, normal modes	University of Georgia Computer Software Mgmt Info Center 382 East Broad Street Athens, GA 30602-4272 Phone: (706) 542-3265 Web: <a href="http://www.cosmic.uga.edu">http://www.cosmic.uga.edu</a>
MSC/PATRAN MSC/NASTRAN MSC/ABAQUS	General pre- and post- processing package Linear statics, dynamics, normal modes, heat transfer Non-linear statics & dynamics	MacNeal Schwindler Corp. 815 Colorado Blvd. Los Angeles, CA 90041-1777 Phone: (800) 336-4858 Web: <a href="http://www.macsch.com">http://www.macsch.com</a>
ANSYS	Linear statics, dynamics, normal modes, heat transfer Highly non-linear statics & dynamics capability	ANSYS, Inc. Southpointe 275 Technology Drive Canonsburg, PA 15317 Phone: (724) 746-3304 Web: <a href="http://www.ansys.com">http://www.ansys.com</a>
I-DEAS	General pre- and post- processing package Linear statics, dynamics, normal modes, heat transfer	Structural Dynamics Research Corp. 2000 Eastman Drive Milford, Ohio 45150-2789 Phone: (513) 576-2400 Web: <a href="http://www.sdrc.com">http://www.sdrc.com</a>
FEMAP	General pre- and post- processing package Linear statics, dynamics, normal modes, heat transfer	Enterprise Software Products, Inc. 415 Eagleview Blvd., Suite 105 Exton, PA 19341 Phone: (610) 458-3660 Web: <a href="http://www.entsoft.com">http://www.entsoft.com</a>
COSMOS	Linear statics, dynamics, normal modes, heat transfer	Structural Research & Analysis Corp. 12121 Wilshire Boulevard, 7th Floor Los Angeles, CA 90025 Phone: (310) 207-2800 Web: <a href="http://www.cosmosm.com">http://www.cosmosm.com</a>

**Table 7-1: Finite element modeling software packages.**

## **VII. Additional Reading**

Timoshenko, S. and Woinowsky-Krieger, Theory of Plates and Shells, 2<sup>nd</sup> edition, New York: McGraw-Hill, 1959

Roark, R. and Young, W., Roark's Formulas for Stress and Strain, 6<sup>th</sup> edition, New York: McGraw-Hill, 1989.

Shigley, J., and Mischke, C., Mechanical Engineering Design, 5<sup>th</sup> edition, New York: McGraw-Hill, 1989.

Blevins, R., Formulas for Natural Frequency and Mode Shape, New York: Van Nostrand Reinhold, 1979.

Newell, J., Larson, T. and Cornford S., "A Thermo-mechanical Stress Analysis of an MCM-D Interconnect," Proceedings of the Pan Pacific Microelectronics Symposium, Honolulu, Hawaii, February 1996.

